Clutter rejection for MTI radar using a single antenna and a long integration time

Philippe Goy*, François Vincent†, Jean-Yves Tourneret‡
*Rockwell-Collins France, 6 avenue Didier Daurat, 31701, Blagnac, France
email: pgoy@rockwellcollins.com
†Department Electronics Optronics and Signal, University of Toulouse/ISAE, Toulouse, France
email: francois.vincent@isae.fr
‡University of Toulouse, IRIT-ENSEEIHT, 2 rue Camichel, Toulouse, France
email: jean-yves.tourneret@enseeiht.fr.

***Abstract*—Moving Target Indicators (MTI) are airborne radar systems designed to detect and track moving vehicles or aircrafts. In this paper, we address the problem of detecting hazardous collision targets to avoid them. One of the best known solutions to solve this problem is given by the so-called Space-Time Adaptive Processing (STAP) algorithms which optimally filter the target signal from interference and noise exploiting the specific relationship between Direction Of Arrival (DOA) and Doppler for the ground clutter. However, these algorithms require an antenna array and multiple reception channels that increase cost and complexity. The authors propose an alternative solution using a single antenna only. In addition to the standard Doppler shift related to the radial speed, the orthoradial speed of any target can be estimated if using a long integration time. Dangerous targets and ground clutter have different signatures in the radial-orthoradial velocity plane. An optimal detector is then proposed based on the oblique projection onto the signal subspace orthogonal to the clutter subspace. The theoretical performances of this detector are derived and a realistic radar scene simulation shows the benefits of this new MTI detector.**

***Index Terms*—MTI Radar, Clutter rejection, oblique projection, long integration time.**

I. Introduction

One of the common goals of airborne radar is to detect and track moving targets. In many practical situations, this detection is heavily degraded by the Doppler spread of the clutter returns due to the platform motion. A well-known solution to cope with this problem is the use of an antenna array, combined with the adopted STAP technique, which adaptively compensates for the Doppler spread of the ground clutter spectrum. In this way, the detector can achieve optimum clutter rejection in the DOA-Doppler space [1]. However, these systems are extremely costly and require heavy processing capacities. Their use is then limited to specific applications. In this paper, we propose an alternative solution using only a single antenna. This new technique can be applied for short or middle range systems and takes advantage of a long integration time to use the Doppler shift variation. Indeed, similarly to Synthetic Aperture Radars (SAR) [2], the Doppler shift cannot be considered constant anymore, and a 2nd order phase component has to be introduced. The first phase component (Doppler frequency shift) is linked to the radial velocity of the target, whereas the 2nd order phase component is linked to the orthoradial velocity. It can be noted that this latter velocity term can also be seen as a DOA variation. In this radial-orthoradial velocity plane, the ground clutter has a very specific signature that will be used for clutter rejection. More precisely, we focus on the problem of airborne detection of hazardous collision targets in order to avoid them. These targets also have a specific signature in the radial-orthoradial velocity plane. Hence, clutter and target belong to two different subspaces. After signal subspace parameter estimation, the optimal detector is derived and analyzed. This detector is the oblique projection onto the signal subspace orthogonal to the clutter subspace.

This paper is organized as follows. The signal model and assumptions are presented in Section 2. In Section 3, after reminding known results about oblique projectors [3], we derive the generalized likelihood ratio (GLR) detector associated with our model. A performance analysis is also conducted. Numerical simulations are provided in Section 4 whereas Section 5 draws conclusions and perspectives.

II. Data Model and Assumptions

We consider an airborne radar embedded on an aircraft flying at constant speed v_a. A possible collision target at range R_0 with constant velocity v_t is heading toward the aircraft up to an impact point, defined by the intersection of both aircraft and target directions. Ground clutter is also present at range R_0, and will compete with the target. Due to long integration time, we have to use a second order Taylor expansion of the target-radar distance [2]

$$R(t) = R_0 + v_r t + \frac{1}{2}\left(a_r + \frac{v_\perp^2}{R_0}\right) t^2 \qquad (1)$$

where R_0 is the initial position of the target, v_r and a_r are the relative radial velocity and acceleration, and $v_\perp$ is the orthoradial velocity. We assume a constant radial velocity such that $a_r = 0$.

After range processing, the returned signal from a target at range R_0 for each pulse repetition m can be written

$$s(m) = Ae^{j\left(a_0 + a_1 m T_r + a_2 m^2 T_r^2\right)} \qquad 0 \leq m \leq M-1 \qquad (2)$$

where Ae^{ja_0} is the target complex amplitude with $a_0 = \frac{4\pi R_0}{\lambda}$, λ is the mean radar wavelength, $a_1 = \frac{4\pi v_r}{\lambda} = 2\pi f_D$ is the linear phase rotation term due to v_r and related to Doppler frequency f_D, $a_2 = \frac{2\pi v_\perp^2}{\lambda R_0} = 2\pi \dot{f}_D$ is the quadratic phase rotation term due to $v_\perp$ and related to Doppler variation $\dot{f}_D$. Note that, due to long integration time T_{int}, relatively short range R_0 and high speed v_a, the term a_2 cannot be neglected in the phase rotation. Although range migration may occur, we make the assumption that this effect is compensated by pre-processing. Of course, the study of chirp signals has received considerable attention in the litterature [4], [5], [6]. This paper exploits specific relationships between parameters a_1 and a_2 for target and clutter leading to an appropriate detector.

A. Collision target model

Let us consider a target heading toward the aircraft with a constant but unknown velocity, as shown in Fig. 1. The target and the aircraft will collide if the aircraft does not change its flying path. This particular situation is characterized by a constant target direction

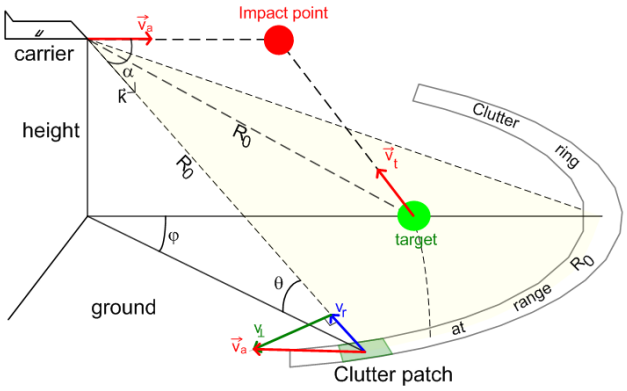

Fig. 1. Ground clutter and collision target at range R_0.

seen from the radar. Therefore, the target has only a radial speed component [7], i.e., $a_2 = 0$, which provides a Doppler signature for collision targets. As a consequence, the radar signal backscattered by the target can be written in the following compact form

$$\boldsymbol{x} = \boldsymbol{h}(a_1)A \tag{3}$$

where $\boldsymbol{h}(a_1) = \left[1, e^{ja_1T_r}, ..., e^{ja_1(M-1)T_r}\right]^T$ is the target Doppler phase evolution, and A is the target complex amplitude.

B. Ground clutter model

Ground clutter is composed by a multitude of local scatterers. The relative velocity of a ground scatterer only depends on the aircraft velocity and on its aspect angle α, hence

$$v_r = v_a \cos\alpha, \quad v_\perp = v_a \sin\alpha.$$

Note that α is a function of elevation θ and azimuth φ through the relation $\cos(\alpha) = \cos(\theta)\cos(\varphi)$. Consequently, the Doppler parameters of any ground clutter source satisfy the same quadratic relation

$$a_2 = \frac{2\pi v_a^2}{\lambda R_0} - \frac{\lambda}{8\pi R_0} a_1^2. \tag{4}$$

All the clutter sources which fall into the same Doppler bin are modeled as one target with complex amplitude B_p and Doppler parameter $a_{1,p}$ such that

$$\boldsymbol{c}_p = B_p \boldsymbol{s}_p \tag{5}$$

where $\boldsymbol{s}_p = \left[1, ..., e^{j(a_{1,p}(M-1)T_r + a_{2,p}(M-1)^2T_r^2)}\right]^T$ is the clutter Doppler phase evolution. Ground clutter is distributed in azimuth (as shown in Fig.1) and is spread over velocities defined by the antenna aperture in azimuth φ_{3dB} and the steering direction (elevation θ and bearing angle φ). The resulting signal, sum of P ground scatterers can be written as follows

$$\boldsymbol{c} = \sum_{p=1}^{P} \boldsymbol{c}_p = \boldsymbol{S}\boldsymbol{B} \tag{6}$$

where the columns of the $M \times P$ complex matrix $\boldsymbol{S}$ contain the generalized Doppler signatures and $\boldsymbol{B}$ is a $P \times 1$ vector containing the complex amplitudes of the clutter sources.

C. Received Radar Signal

After range processing, the received signal is composed of the components due to the collision target $\boldsymbol{h}A$, the ground clutter sources $\boldsymbol{S}\boldsymbol{B}$, and an additive white Gaussian noise vector $\boldsymbol{w}$

$$\boldsymbol{y} = \boldsymbol{h}A + \boldsymbol{S}\boldsymbol{B} + \boldsymbol{w}. \tag{7}$$

This linear model has received much attention in signal processing (e.g., [3], [8],[9], [10]), where $\boldsymbol{h}$ and $\boldsymbol{S}$ define a signal subspace and an interference subspace respectively. We assume in this study that A and $\boldsymbol{B}$ are constant over integation time and deterministic. Note that A and $\boldsymbol{B}$ can be considered Gaussian instead, but [11] showed that, when interference dominates noise, the solutions in the stochastic case converge to the solutions in the determinstic case. As clutter often dominates noise, the deterministic assumption is not too restrictive. Note that the proposed model differs from [3], [8], since $\boldsymbol{h}$ depends on the unknown quantity a_1, and that the proposed model can be extended to multiple targets (see also Fig.2 for example).

III. ESTIMATION AND DETECTION

This section derives the Maximum Likelihood (ML) estimator of the Doppler frequency shift for the target of interest as well as the associated Generalized Likelihood Ratio Test (GLRT). Optimal estimation and detection using model (7) require oblique projection as stated in [3], [8],.

A. Estimation

The ML estimator for the unknown parameters A, $\boldsymbol{B}$ and a_1 from the vector of observations $\boldsymbol{y}$ is derived from the negative log-likelihood function

$$J(A, \boldsymbol{B}, a_1) = \|\boldsymbol{y} - \boldsymbol{h}(a_1)A - \boldsymbol{S}\boldsymbol{B}\|^2 \tag{8}$$

where $\|\boldsymbol{x}\|^2 = \boldsymbol{x}^*\boldsymbol{x}$ and * is the transpose conjugate operator. For any value of a_1, the parameters A and $\boldsymbol{B}$ minimizing the negative log-likelihood have been derived in [3]. The solutions are oblique pseudo-inverse projections :

$$\hat{A} = \left(\boldsymbol{h}^*\boldsymbol{P}_{\boldsymbol{S}}^{\perp}\boldsymbol{h}\right)^{-1}\boldsymbol{h}^*\boldsymbol{P}_{\boldsymbol{S}}^{\perp}\boldsymbol{y} = \left(\boldsymbol{P}_{\boldsymbol{S}}^{\perp}\boldsymbol{h}\right)^{+}\boldsymbol{y} \tag{9}$$

$$\hat{\boldsymbol{B}} = \left(\boldsymbol{S}^*P_{\boldsymbol{h}}^{\perp}\boldsymbol{S}\right)^{-1}\boldsymbol{S}^*P_{\boldsymbol{h}}^{\perp}\boldsymbol{y} = \left(P_{\boldsymbol{h}}^{\perp}\boldsymbol{h}\right)^{+}\boldsymbol{y} \tag{10}$$

where $^+$ denotes the Moore-Penrose pseudo-inverse operator and $\boldsymbol{P}_{\boldsymbol{S}}^{\perp} = I_M - \boldsymbol{S}\left(\boldsymbol{S}^*\boldsymbol{S}\right)^{-1}\boldsymbol{S}^*$ is the orthogonal projection on subspace $<S>^{\perp}$, and I_M is the $M \times M$ identity matrix. After replacing A and $\boldsymbol{B}$ by their ML estimates in the negative log-likelihood, we obtain the following criterion

$$J\left(\hat{A}, \hat{\boldsymbol{B}}, a_1\right) = \|\boldsymbol{y} - \boldsymbol{h}(a_1)\hat{A} - \boldsymbol{S}\hat{\boldsymbol{B}}\|^2.$$

If we introduce the data projection onto $<\boldsymbol{S}>^{\perp}$, we otbtain

$$\tilde{\boldsymbol{y}} = \boldsymbol{P}_{\boldsymbol{S}}^{\perp}\boldsymbol{y} = \boldsymbol{P}_{\boldsymbol{S}}^{\perp}\boldsymbol{h}A + \boldsymbol{P}_{\boldsymbol{S}}^{\perp}\boldsymbol{w}.$$

The negative log-likelihood of the projected data $\tilde{\boldsymbol{y}}$ provides the following criterion

$$J\left(\hat{A}, a_1\right) = \|\tilde{\boldsymbol{y}} - \tilde{\boldsymbol{h}}\hat{A}\|^2 = \tilde{\boldsymbol{y}}^*\tilde{\boldsymbol{y}} - \tilde{\boldsymbol{y}}^*\boldsymbol{h}\left(\boldsymbol{h}^*\boldsymbol{P}_{\boldsymbol{S}}^{\perp}\boldsymbol{h}\right)^{-1}\boldsymbol{h}^*\tilde{\boldsymbol{y}}. \tag{11}$$

Thus the ML estimator of a_1 is

$$\hat{a}_1 = \arg\max_{a_1} \boldsymbol{y}^*\boldsymbol{P}_{\boldsymbol{S}}^{\perp}\boldsymbol{h}\left(\boldsymbol{h}^*\boldsymbol{P}_{\boldsymbol{S}}^{\perp}\boldsymbol{h}\right)^{-1}\boldsymbol{h}^*\boldsymbol{P}_{\boldsymbol{S}}^{\perp}\boldsymbol{y} \tag{12}$$

or equivalently

$$\hat{a}_1 = \arg\max_{a_1} \boldsymbol{y}^*\boldsymbol{P}_{\boldsymbol{S}}^{\perp}\boldsymbol{P}_{\boldsymbol{P}_{\boldsymbol{S}}^{\perp}\boldsymbol{h}(a_1)}\boldsymbol{P}_{\boldsymbol{S}}^{\perp}\boldsymbol{y} \tag{13}$$

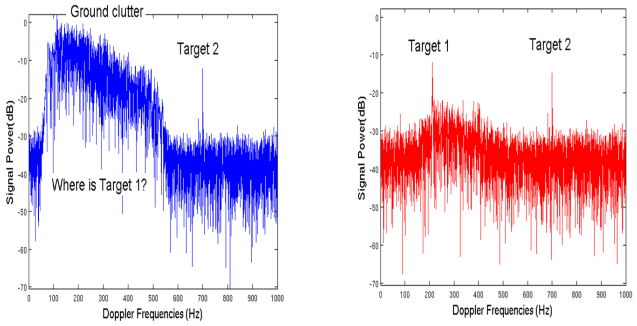

(a) FFT (b) Oblique projection

Fig. 2. FFT and oblique projection for the received signal.

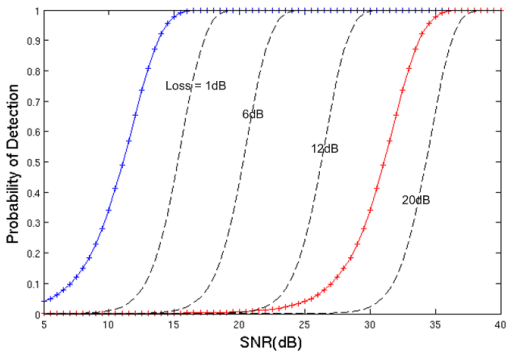

Fig. 3. Probability of detection as a function of SNR

where $\boldsymbol{P}_{\boldsymbol{P}_{\boldsymbol{S}}^{\perp}h}$ is the orthogonal projection on subspace $<\boldsymbol{P}_{\boldsymbol{S}}^{\perp}\boldsymbol{h}>$. The data are projected onto $<\boldsymbol{S}>^{\perp}$ to suppress the clutter before being maximized by the projection onto $<\boldsymbol{P}_{\boldsymbol{S}}^{\perp}\boldsymbol{h}>$.

B. Detection

The target detection problem can be expressed by the following binary hypothesis testing problem

$$\begin{aligned}&\mathcal{H}_0(\text{absence of target}) : \boldsymbol{y} \sim \mathcal{CN}(\boldsymbol{SB}, \sigma^2 I_M),\\ &\mathcal{H}_1(\text{presence of a target}) : \boldsymbol{y} \sim \mathcal{CN}(\boldsymbol{h}A + \boldsymbol{SB}, \sigma^2 I_M),\end{aligned} \tag{14}$$

where I_M is the $M\times M$ identity matrix. As parameter a_1 is unknown, there are two ways of proceeding. One possibility is to apply the GLR detector of [8] (derived for known a_1 and unknown A, B and σ^2) for all possible values of a_1

$$L(a_1) = \frac{\boldsymbol{y}^* \boldsymbol{P}_{\boldsymbol{S}}^{\perp} \boldsymbol{P}_{\boldsymbol{P}_{\boldsymbol{S}}^{\perp}\boldsymbol{h}(a_1)} \boldsymbol{P}_{\boldsymbol{S}}^{\perp} \boldsymbol{y}}{\boldsymbol{y}^* \boldsymbol{P}_{\boldsymbol{S}}^{\perp} \left(I - \boldsymbol{P}_{\boldsymbol{P}_{\boldsymbol{S}}^{\perp}\boldsymbol{h}(a_1)}\right) \boldsymbol{P}_{\boldsymbol{S}}^{\perp} \boldsymbol{y}}. \tag{15}$$

Note that the detectors of [8] were derived in the real data case and that the generalization to complex data was given in [11]. The second possibility is the so-called GLRT which consists in estimating a_1 by ML maximization and replacing $\hat{a}_1$ in the likelihood ratio. As shown in (13), $\hat{a}_1$ is obtained by maximizing the test statistics in (15), and the GLRT is the same as (15). Instead of calculating the entire detector for all a_1, we can then calculate (13) for each a_1, find its maximum value, and apply the division in (15) to get the detector for $\hat{a}_1$. In our single target case, this processing is optimal and less computation consuming. However, if the number of target is unknown, a systematic search for all possible a_1 is needed.

C. Performance analysis

False alarm rate and detection probability have closed form expressions defined by [8]

$$\begin{aligned}P_{\text{fa}} &= 1 - F_{2p,2(s-p),0}(\eta)\\ P_d &= 1 - F_{2p,2(s-p),\Lambda^2}(\eta)\end{aligned}$$

where η is the detection threshold and $F_{2p,2(s-p),\Lambda^2}(.)$ is the cumulative distribution function of a noncentral F distribution with parameters $2p$, $2(s-p)$ and non-centrality parameter $\Lambda^2 = \frac{|A|^2}{\sigma^2}\|\boldsymbol{P}_{\boldsymbol{S}}^{\perp}\boldsymbol{h}\|^2$. Note that s is the rank of $\boldsymbol{S}$, $p=1$ is the rank of $\boldsymbol{h}$ and Λ^2 represents the output SNR after pre-processing by $\boldsymbol{P}_{\boldsymbol{S}}^{\perp}$. Note that, compared to the maximum processing gain M, the quantity $\|\boldsymbol{P}_{\boldsymbol{S}}^{\perp}h\|^2$ can be seen as a processing loss due to oblique projection. These statistics allow Receiver Operating Curves (ROC) to be computed.

IV. Simulation Results

In this section, we first apply our processing on simulated radar data and derive some requirements for the processing to be effective. We then conclude by testing our processing on real airborne radar clutter data.

A. Simulation

In this section, we consider the following scenario defined by a mean radar wavelength $\lambda = 3cm$ and an azimuth aperture of $\varphi_{3dB} = 40^\circ$. The aircraft flies at a constant velocity $v_a = 65ms^{-1}$ at height $h = 500m$ above the ground, and looks forward with an elevation angle θ=25° as presented in Fig.1. A target is approaching the aircraft at range $R_0 = 1200m$ with velocity $v_t = 35ms^{-1}$. Its aspect angle is constant and equals $\alpha = 30^\circ$. The corresponding collision time is $T_c = 13.8s$. The radar pulse repetition frequency is PRF $= 1kHz$ which corresponds to an ambiguous speed of $v_{\text{amb}} = \lambda.\text{PRF}/2 = 15ms^{-1}$. The radial velocity of the collision target is $v_r = -RT_c^{-1} = 2.8ms^{-1}\text{mod}[v_{\text{amb}}]$, where mod$[v_{\text{amb}}]$ stands for "modulo v_{amb}". Note that the target is in the same Doppler region as the ground, as the minimum and maximum clutter velocities are respectively $v_{min} = -v_a\cos(\theta)\cos(\frac{\varphi_{3dB}}{2}) = 4.5ms^{-1}\text{mod}[v_{\text{amb}}]$, $v_{max} = -v_a\cos(\theta) = 1ms^{-1}\text{mod}[v_{\text{amb}}]$. We also consider a second target located outside the clutter region. Its properties are the same as for the collision target except that its aspect angle is 19° and its relative velocity is $10.5ms^{-1}\text{mod}[v_{\text{amb}}]$. The ground clutter Radar Cross Section (RCS) follows a constant gamma rule as in [2]: RCS $= \sigma_0 R\Delta\varphi\Delta R$, where $\sigma_0 = \gamma\sin\theta$ and $\Delta\varphi, \Delta R$ are the dimensions in azimuth and range of the Range-Doppler bin. Target RCS are $-10dB$ under the minimum ground RCS. Finally, the integration time is set to $T_{\text{int}} = 4s$ in order to obtain a post-processing signal to noise ratio of $\text{SNR}_o = 20\text{dB}$.

We first compare our new processing to the common Doppler processing defined by a simple Fast Fourier Transform (FFT) in Fig. 2. In the first scenario denoted as (a), an FFT is applied to $\boldsymbol{y}$, and we can see that one target falls outside the clutter whereas the other one is hidden by the clutter and cannot be detected. In scenario (b), the new processing based on oblique projections is applied according to (9) for each possible Doppler frequency. Thanks to clutter suppression, both targets appear clearly and can be detected with a sufficient SNR, ensuring a good false alarm rate.

Figure 3 shows in dotted lines the detection probability P_{d} of the proposed detector as a function of SNR for a false alarm probability P_{fa}=10^{-6} and for different processing losses due to $\|\boldsymbol{P}_{\boldsymbol{S}}^{\perp}h\|^2$. Note that the clutter-to-noise ratio is $20dB$. Comparatively, solid lines

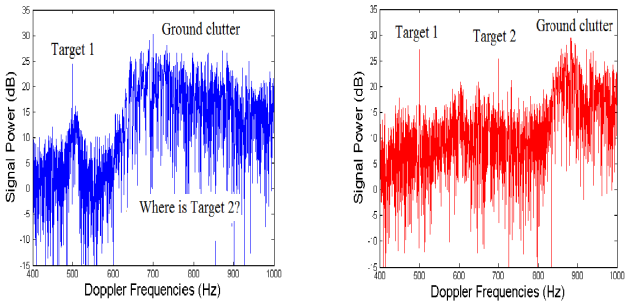

(a) FFT (b) Oblique projection

Fig. 4. FFT and oblique projection for real clutter data

represent a detector obtained by FFT processing and a cell averaging constant false alarm rate detection (the blue line corresponds to a target located outside clutter whereas the target is inside clutter for the red line). These results show that the target detector performance depends on how much the target energy is located outside the clutter subspace, i.e., on $\|\boldsymbol{P}_{\boldsymbol{S}}^{\perp} h\|^2$. A small value of this energy results in a small value of Λ^2, for any SNR $= \frac{|A|^2}{\sigma^2}$, resulting in poor detection performance. This situation occurs when the integration time or the aircraft velocity is not high enough, or for higher range.

B. Discussion

The performance of the proposed detector depends on the quantity $\|\boldsymbol{P}_{\boldsymbol{S}}^{\perp}\boldsymbol{h}\|^2$ which determines its ability to suppress clutter without reducing the target echo. It measures how much the target is separated from the ground clutter and can be interpreted in terms of principal angle between signal and clutter subspaces, i.e., in terms of $\|\boldsymbol{P}_{\boldsymbol{S}}^{\perp}\boldsymbol{h}\|^2 = N\sin^2(\beta)$, where N is the number of processing points and β is the principal angle [3]. To maximize this criterion, one has to increase integration time in order to have a significant quadratic phase evolution to separate clutter and target. Moreover this second order term will be maximized for small range and high speed applications. However, when the clutter region can be seen with low elevation at the same range than the target, i.e., with a low aspect angle, the clutter can also become a collision target and cannot be separated anymore from other targets.

C. Airborne Radar Clutter Data

We now test our processing on real clutter data, obtained by a forward-looking airborne X-band radar. The goal is primarily to test the clutter rejection capability of our processing, as no real target is present in the data set. Two synthetic targets are added to the clutter data set, one is placed outside clutter and the other one is placed inside main lobe clutter. The observed initial range is $850m$. Carrier velocity and height are approximately $65ms^{-1}$ and $350m$. The integration time is about $4s$, and migration has been compensated by pre-processing for main lobe clutter. Note that the radar antenna beam in azimuth is much wider than for the simulated data, and that other ground echoes are originated from secondary antenna lobes in real situation. Consequently, sidelobes clutter echoes are present in the signal, and their migration cannot be compensated by pre-processing along with the migration of the main lobe clutter.

As for simulated data, FFT and the proposed strategy are compared in Fig. 4. In scenario (a), FFT is applied to the real clutter data, and we can see the first synthetic target outside the clutter whereas the other one is hidden by clutter. In scenario (b), the new processing is applied. Main lobe clutter is successfully rejected and the second synthetic target appears. The processing gain on SINR (Signal to Interference Plus Noise Ratio) is then between 15 and 20dB. Note that the matrix S has been constructed using the main lobe of the antenne only. As a consequence, there is remaining clutter observed in the right part of Fig.4b resulting from antenna sidelobes.

V. Conclusion

This paper presented a new MTI detector for airborne radar using a single antenna. More precisely, we focused on the detection of collision targets in the presence of ground clutter for short or middle range applications. The clutter was suppressed using a long integration time and exploiting the characteristic signature of its phase evolution. Indeed, clutter belongs to a given subspace defined by the relation between radial and orthoradial speeds of all fixed targets. Dangerous targets are characterized by a different signature where the second order phase parameter (Doppler variation) is null. This problem of detecting a signal belonging to a partly known subspace in presence of known interferences was solved using oblique projections. The performance of the detector was provided, and numerical radar simulations attest to the validity of this new MTI detector. The best performance increase will be obtained for short range and high speed applications. Future work includes extension of the proposed detector for non-gaussian clutter and time-varying amplitudes.

References

[1] R. Klemm, *Principles of Space-Time Adaptive Processing*, IEE Press, London, U.K., 2002.

[2] P. Lacomme, *Air and Spaceborne Radar Systems*, William Andrew Scitech Publishing, Norwich, NY, 2001.

[3] R. T. Behrens and L. L. Scharf, "Signal processing applications of oblique projection operators," *IEEE Trans. Signal Process.*, vol. 42, no. 6, pp. 1413–1424, June 1994.

[4] P. M. Djuric and S. M. Kay, "Parameter estimation of chirp signals," *IEEE Trans. Acoustic, Speech and Signal Process.*, vol. 38, no. 12, pp. 2118–2126, 1990.

[5] F. Gini, M. Montanari, and L. Verrazzani, "Estimation of chirp radar signals in compound-gaussian clutter: a cyclostationnary approach," *IEEE Trans. Signal Process.*, vol. 48, no. 4, pp. 1029–1039, 2000.

[6] Y. Sun and P. Willett, "Hough transform for long chirp detection," *IEEE Trans. Aerospace and Electronic Systems*, vol. 38, no. 2, pp. 533–569, 2002.

[7] S. Kemkemian, M. Nouvel-Fiani, P. Cornic, P. Le Bihan, and P. Garrec, "Radar systems for "Sense and Avoid" on UAV," in *Proc. Int. Rad. Conf. on Surveillance for a Safer World*, Bordeaux, France, 2009.

[8] L. L. Scharf and B. Friedlander, "Matched subspace detectors," *IEEE Trans. Signal Process.*, vol. 42, no. 8, pp. 2146–2157, Aug. 1994.

[9] R. Boyer and G. Bouleux, "Oblique projections for direction-of-arrival estimation with prior knowledge," *IEEE Trans. Signal Process.*, vol. 56, no. 4, pp. 1374–1387, Dec. 2008.

[10] O. Besson, L. L. Scharf, and F. Vincent, "Matched direction detectors and estimators for array processing with subspace steering vector uncertainties," *IEEE Trans. Signal Process.*, vol. 53, no. 12, pp. 4453–4463, 2005.

[11] L. L. Scharf and M. L. McCloud, "Blind adaptation of zero forcing projections and oblique pseudo-inverses for subspace detection and estimation when interference dominates noise," *IEEE Trans. Signal Process.*, vol. 50, no. 12, pp. 2938–2946, Dec. 2002.